International Journal on Electrical Engineering and Informatics - Volume 17, Number 2, June 2025

Design and Experimental Validation of a Particle Filter-Based Navigation System for a Hybrid Autonomous Underwater Glider

Natsir Habibullah[1], Bambang Riyanto Trilaksono[2], Egi Muhammad Idris Hidayat[2], Widyawardana Adiprawita[2] and Simon Siregar[3]

[1]Doctoral Program of Electrical Engineering and Informatics
[1,2]School of Electrical Engineering and Informatics, Institut Teknologi Bandung
[3]Department of Computer Engineering, Faculty of Applied Science, Telkom University
Bandung, Indonesia
[1]nhabibullah@unib.ac.id

Abstract: This paper presents the design, implementation, and experimental validation of a navigation system for a Hybrid Autonomous Underwater Glider (HAUG) using a Particle Filter framework. The system integrates data from an Inertial Measurement Unit (IMU), Doppler Velocity Log (DVL), depth sensor, and GPS to estimate the vehicle's position and velocity, particularly during submerged operations where GPS signals are unavailable. Sensor data were processed through calibration and low-pass filtering to improve accuracy. The navigation algorithm was designed using a sequential Monte Carlo approach, with modules for particle initialization, propagation based on IMU input, and conditional resampling using available DVL, depth, and GPS data. The proposed algorithm incorporates adaptive resampling and particle rejuvenation strategies to enhance robustness under limited sensor observability. The system was tested in both controlled pool trials and open-sea environments, including dive-glide maneuvers and surface transit scenarios. The results demonstrate that the particle filter-based system can provide consistent position and velocity estimates, even under GPS-denied conditions. Although no ground-truth comparison was available, the performance analysis based on sensor consistency and behavior during dynamic transitions validates the feasibility of the proposed method. This work contributes to the development of robust and adaptable navigation solutions for energy-constrained, hybrid underwater platforms operating in real-world environments.

Keywords: Hybrid Autonomous Underwater Glider (HAUG); Particle Filter; Underwater Navigation; Sensor Fusion; GPS-Denied Localization; Doppler Velocity Log; IMU; Depth Sensor.

1. Introduction

Hybrid Autonomous Underwater Gliders (HAUGs) represent a novel class of underwater vehicles that combine the low-energy buoyancy-driven propulsion of gliders with the maneuverability and control of conventional Autonomous Underwater Vehicles (AUVs). This hybridization allows HAUGs to perform long-duration missions with minimal power consumption while maintaining the ability to maneuver effectively in complex underwater environments. These capabilities make HAUGs highly suitable for a broad range of applications, including oceanographic research, environmental monitoring, seabed mapping, and maritime surveillance, particularly in remote or GPS-denied areas.

The effectiveness of HAUGs in such missions is critically dependent on the accuracy and reliability of their navigation systems. Unlike surface or aerial vehicles that have continuous access to Global Positioning System (GPS) signals, underwater vehicles lose GPS connectivity once submerged. In the absence of GPS, HAUGs must rely on alternative sensor modalities—such as Inertial Measurement Units (IMUs), Doppler Velocity Logs (DVLs), and depth sensors—to estimate their position, orientation, and velocity. However, each of these sensors is prone to specific limitations. IMUs suffer from integration drift and bias, DVLs may lose bottom-lock depending on seabed conditions, and depth sensors only provide partial state

Received: May 9th, 2025. Accepted: June 25th, 2025
DOI: 10.15676/ijeei.2025.17.2.2

information. Fusing these data sources in a reliable and computationally efficient manner is a core challenge for underwater navigation.

Recent advancements in underwater navigation have introduced various estimation techniques to overcome the limitations of dead reckoning and purely inertial systems. Kalman Filter-based approaches, such as the Extended Kalman Filter (EKF) and Unscented Kalman Filter (UKF), have been widely adopted for fusing data from IMUs, DVLs, and depth sensors, particularly for conventional AUVs [1], [2],. However, these filters assume linear dynamics and Gaussian noise, which may not hold in real-world underwater conditions. To address such challenges, Particle Filters have been explored as an alternative due to their robustness in handling nonlinear models and non-Gaussian uncertainties [3], [4]. Applications of Particle Filters include sonar-based localization [5], terrain-aided navigation [6], and integration with acoustic communication systems [7]. Despite these developments, most implementations remain focused on conventional AUVs or simulation-based environments. The use of Particle Filters in hybrid underwater platforms such as HAUGs, particularly with real-time sensor integration and field validation, remains limited and presents a significant research opportunity. In this study, we propose the design and implementation of a real-time navigation system for a Hybrid Autonomous Underwater Glider using a Particle Filter-based framework. The proposed system fuses data from four key sensors: an IMU for motion and orientation estimation, a DVL for velocity, a depth sensor for vertical positioning, and a GPS receiver for position correction when the vehicle surfaces. The Particle Filter algorithm operates through sequential steps of initialization, propagation based on vehicle dynamics, and resampling guided by sensor measurements, adjusting its behavior based on the availability of GPS, DVL, and depth data.

The main contributions of this paper are threefold: (1) the integration of a sequential Monte Carlo-based Particle Filter algorithm into a real-time navigation system for HAUGs, (2) the validation of this system through experimental testing in both controlled (pool) and natural (coastal) environments, and (3) the performance analysis of the navigation output under GPS-denied and GPS-available scenarios without relying on ground-truth positioning systems. The findings support the feasibility of using Particle Filter-based navigation for hybrid underwater vehicles and provide a basis for further advancements in autonomous marine systems operating in uncertain and unstructured underwater environments.

2. Fundamental Theory

The development of a reliable navigation system for Hybrid Autonomous Underwater Gliders (HAUGs) requires a firm theoretical foundation that combines vehicle kinematics, sensor characteristics, and robust state estimation algorithms. This section outlines the core theories used in designing the navigation framework, including the vehicle’s kinematic model, the physical principles and limitations of key sensors, and the implementation of a Particle Filter-based estimation algorithm. These theoretical components provide the basis for integrating multi-sensor data in real-time for underwater localization in GPS-denied environments.

A. Kinematic Model of the Underwater Vehicle

The motion of an autonomous underwater vehicle (AUV), including hybrid variants such as HAUGs, is described using two reference frames: the inertial Earth-fixed frame and the body-fixed frame attached to the vehicle. The Earth frame is typically defined in a North-East-Down (NED) coordinate system, whereas the body frame moves with the vehicle and is aligned with its principal axes of motion. All positions are expressed in the NED (North-East-Down) Earth-fixed frame, while velocity and orientation are defined in the vehicle's body-fixed XYZ frame. Let the state vector $\boldsymbol{\eta} = [x, y, z, \phi, \theta, \psi]^T$ represent the vehicle's position (x, y, z) and orientation in terms of roll (ϕ), pitch (θ), and yaw (ψ). The body-frame velocity vector is defined as $\nu = [u, v, w, p, q, r]^T$, representing linear (u, v, w) and angular (p, q, r) velocities.

The transformation between these two frames is governed by the nonlinear kinematic equation [8]:

$$\dot{\boldsymbol{\eta}} = \boldsymbol{J}(\boldsymbol{\eta})\boldsymbol{v}$$

where $J(\eta)$ is the transformation matrix combining translational and rotational components derived from Euler angles. This model forms the basis for vehicle motion propagation in the estimation process. Due to the nonlinear nature of these dynamics, especially during combined diving and gliding maneuvers, conventional linear filters are often inadequate, necessitating the use of more flexible estimation techniques.

B. Sensor and The Limitations

Underwater navigation without continuous access to GPS relies heavily on integrating multiple onboard sensors. Each sensor provides partial, noisy, and sometimes unreliable information about the vehicle's state. A robust estimation framework must account for the unique limitations and error characteristics of each.

- Inertial Measurement Unit (IMU): IMUs provide high-frequency measurements of linear acceleration and angular velocity along three axes. By integrating these values over time, estimates of velocity, position, and orientation can be obtained. However, IMUs are prone to cumulative errors due to sensor drift, bias, and random walk noise, which degrade estimation accuracy over time [9].
- Doppler Velocity Logger (DVL): The DVL uses acoustic Doppler shift to estimate the vehicle's velocity relative to the seafloor. It can provide accurate velocity measurements in three axes when bottom-lock is maintained, typically at depths of less than 200 meters and over solid seabeds. DVL data may become unreliable in areas with soft sediment or steep terrain [10].
- Depth Sensor: Depth sensors (based on pressure transducers) offer reliable vertical position measurements by estimating hydrostatic pressure. They are generally robust and accurate, but provide only one-dimensional position data [11], [12].
- Global Positioning System (GPS): GPS provides absolute position information but is only available when the vehicle surfaces or operates near the surface. Underwater, GPS data becomes unavailable due to signal attenuation. Therefore, GPS is typically used for intermittent correction of accumulated drift [13], [14].

The successful fusion of these sensors requires compensating for their individual limitations while leveraging their strengths. This is achieved through probabilistic estimation methods such as Particle Filters.

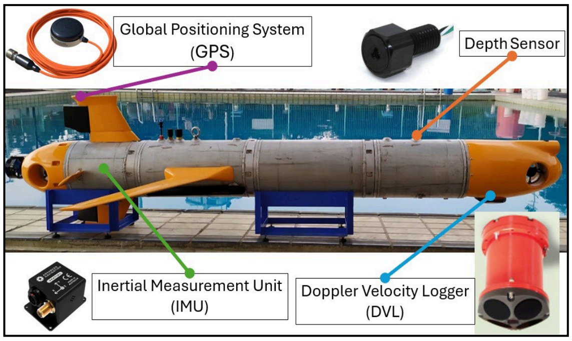

Figure 1. Sensors placement on the vehicle

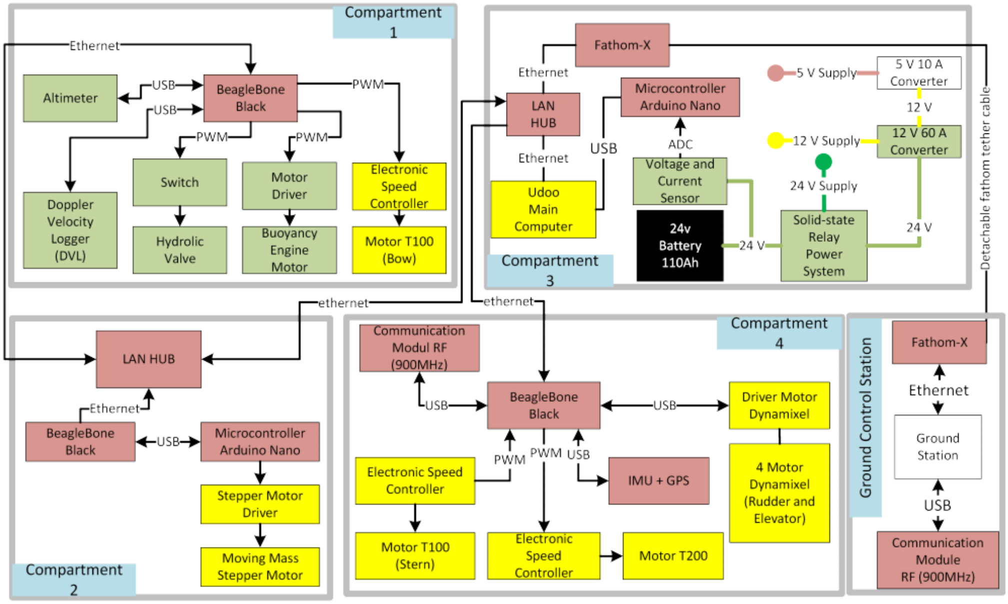

Figure 2. Block diagram and electrical component of the HAUG [15]

C. Particle Filter

The Particle Filter (PF), also known as the Sequential Monte Carlo (SMC) method, is a sampling-based recursive Bayesian estimator that approximates the posterior distribution of a system's state using a set of random weighted samples (particles). It is particularly effective for systems characterized by nonlinear dynamics and non-Gaussian noise, such as underwater navigation scenarios [16]. A typical PF operates in four main stages:

- Initialization: A set of particles $\{x_i^0\}_{i=1}^N$ is sampled from an initial probability distribution. Each particle x_i represents a possible hypothesis of the vehicle's state and is assigned an initial weight w_i^0, typically uniform.
- Prediction (Propagation): Each particle is propagated forward using the motion model, which in this context includes integrating IMU-derived acceleration and orientation using the vehicle's kinematic equations. This models the natural dynamics of the vehicle under the influence of buoyancy and thrust [17].
- Update (Measurement Weighting): Weights of each particle are updated based on the likelihood of observing the current sensor measurements (e.g., from DVL, depth sensor, GPS) given the particle's predicted state. This likelihood is computed using sensor models that account for measurement uncertainty [4].
- Resampling: Particles with low weights are discarded and replaced with copies of particles with higher weights. This step mitigates particle degeneracy and concentrates computational resources on the most probable state hypotheses.

The PF offers several advantages over traditional filters. Unlike Kalman Filters, which rely on linear Gaussian assumptions, Particle Filters do not require analytical expressions for the posterior distribution. They are therefore highly flexible and can accommodate complex motion models and intermittent sensor updates.

D. Relevance to HAUG Navigation

In the context of HAUG operations, the use of Particle Filters allows the navigation system to remain robust even when certain sensor data is temporarily unavailable or unreliable. For example, the vehicle can continue estimating its position during submersion by propagating IMU data, and then resample or correct its state when GPS becomes available upon surfacing.

Similarly, intermittent DVL data can be selectively fused to correct drift when bottom-lock is achieved. This ability to dynamically adapt to varying sensor availability is critical in hybrid glider operations where energy constraints and ocean conditions limit continuous high-fidelity sensing.

3. Sensor Validation and Data Conditioning Experiments

This section presents a set of experimental evaluations aimed at validating the sensor suite integrated into the Hybrid Autonomous Underwater Glider (HAUG). The objective is to assess the behavior, accuracy, and limitations of each sensor in practical environments, as well as to identify appropriate data conditioning strategies that enable robust fusion within the particle filter-based navigation system.

A. Experimental Setup

Two experimental campaigns were conducted to validate the performance of the onboard sensors under different operational conditions: a controlled environment and a real-world coastal setting.

- Pool Testing: Conducted in the Saraga outdoor diving pool (15 × 15 meters, 4–5 meters depth), this campaign allowed for systematic evaluation under known and repeatable conditions. The HAUG performed surface maneuvers and gliding dives while sensor readings were collected. The still water and controlled setup helped isolate specific behaviors of each sensor during transitions, particularly when analyzing disturbances caused by thruster activation or attitude changes.
- Field Testing: To examine the system's real-world performance, open-water trials were performed at Pangandaran Beach. This environment introduced natural disturbances such as ocean currents, surface waves, and signal attenuation. It also allowed the team to assess sensor dropout (particularly GPS) during submerged phases and reacquisition upon resurfacing, replicating conditions encountered during actual deployments.

In both tests, the HAUG was equipped with:

- An IMU for acceleration and orientation, sampled at 40 Hz.
- A DVL for bottom-relative velocity, sampled at 1 Hz.
- A GPS receiver for surface position fixes, sampled at 40 Hz.
- A Depth Sensor for vertical position, sampled at 10 Hz.

Two motion scenarios were evaluated:

- Surface Yaw Maneuver: The vehicle executed controlled changes in heading while maintaining forward movement at the surface.
- Submersion and Recovery: The vehicle dived to a depth of approximately 3.5 meters before returning to the surface.

Sensor data from both campaigns were logged and analyzed to observe accuracy, latency, signal noise, and dropouts, with comparisons made between both environments.

B. Surface Motion Test Results

During the surface yaw maneuver scenario (see Fig. 3), the HAUG was commanded to adjust its heading incrementally while maintaining a constant forward velocity. This test aimed to evaluate the performance of key onboard sensors—IMU, GPS, DVL, and depth sensor—during horizontal motion at the water surface in an outdoor pool.

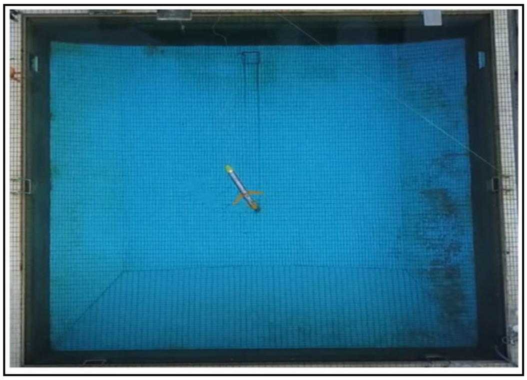

Figure 3. Pool testing at Saraga diving pool

The Inertial Measurement Unit (IMU) consistently captured yaw changes corresponding to the control inputs (see Fig. 4). The yaw angle followed a stepped profile as expected, although minor oscillations were observed after each command, likely due to inertia and minor hydrodynamic resistance. Pitch and roll angles remained relatively stable, but a consistent roll bias of approximately 13° was observed (see Fig. 5). This offset may result from misalignment in sensor installation or internal drift and was later corrected via calibration.

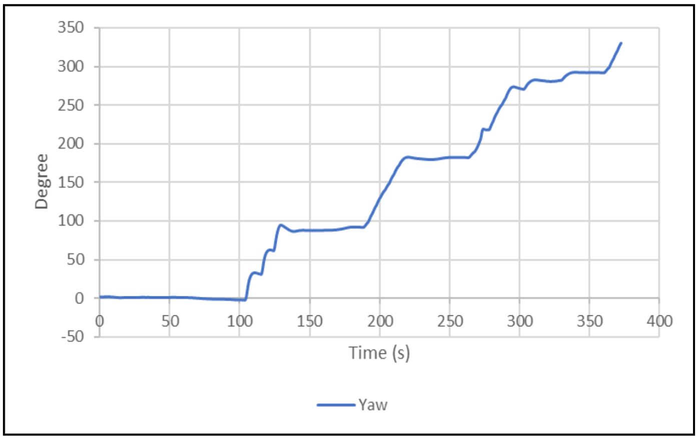

Figure 4. Yaw angle at surface yaw maneuver scenario

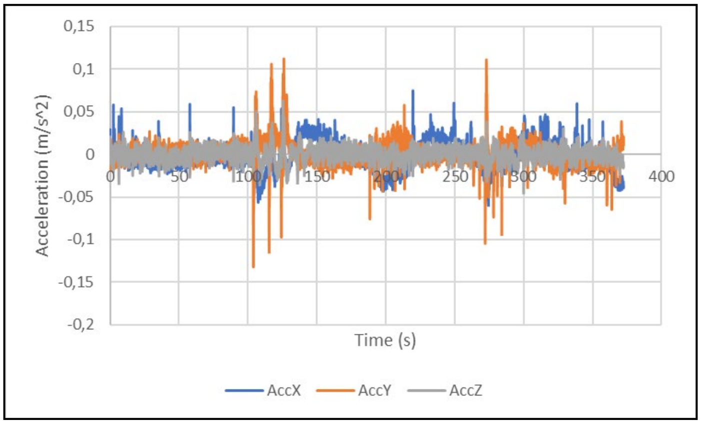

Figure 5. Roll and pitch angle at surface yaw maneuver scenario

The GPS receiver, sampled at 40 Hz, delivered continuous and consistent positioning updates throughout the surface motion (see Fig. 6). The reported coordinates matched the vehicle's actual trajectory, and the system maintained a low covariance index, indicating a strong satellite lock. GPS data served as a benchmark for evaluating Particle Filter corrections and was considered highly reliable for surface operations.

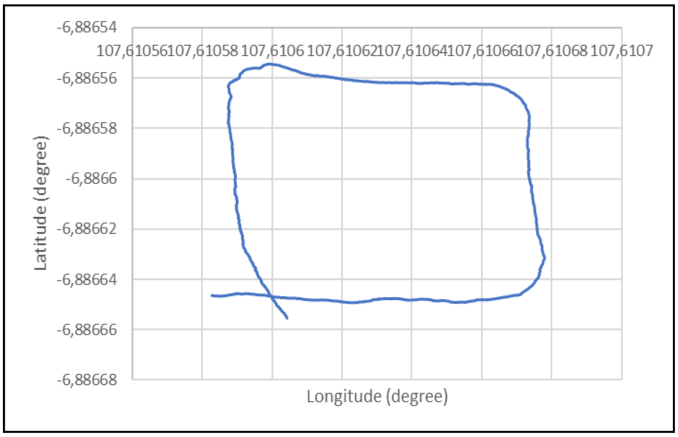

Figure 6. GPS's coordinate measurement at surface yaw maneuver scenario

The Doppler Velocity Log (DVL) recorded body-frame velocities aligned with the forward motion of the vehicle (see Fig. 7). In this shallow environment, bottom-lock was mostly maintained, though the output showed significant high-frequency noise. This noise was mitigated through low-pass filtering, which allowed extraction of a reliable horizontal velocity profile. The velocity data confirmed that the vehicle maintained a steady thrust level throughout the yaw maneuver.

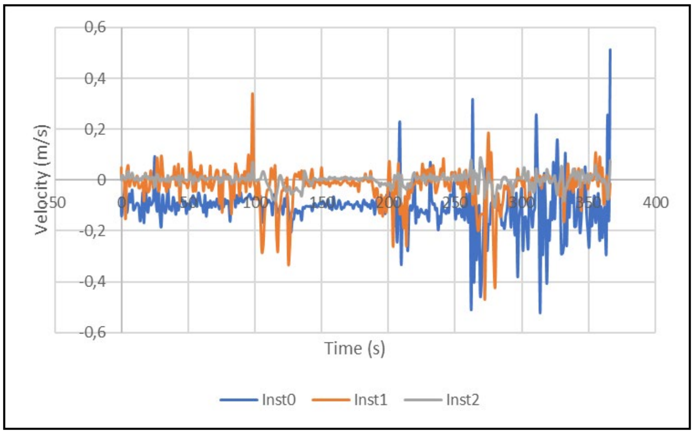

Figure 7. DVL's velocity measurement at surface yaw maneuver scenario

The depth sensor, expected to read close to zero at the surface, consistently reported an offset of approximately −1 meter (see Fig. 8). This offset remained relatively stable and was later used to recalibrate the depth baseline using verified GPS-surface points. The discrepancy was attributed to either initial calibration error or pressure offset at the water surface.

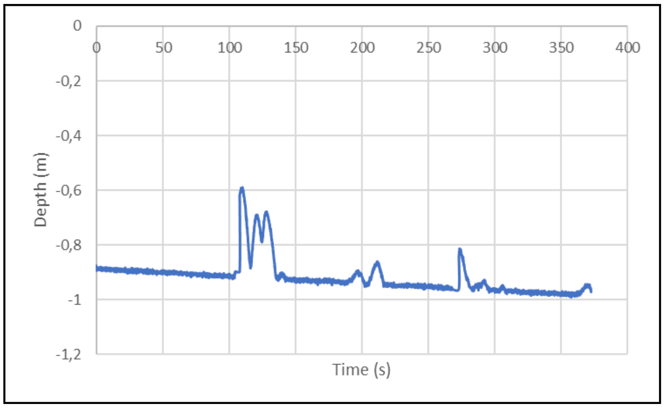

Figure 8. Depth measurement at surface yaw maneuver scenario

These results highlight that while each sensor provided valuable insights, they also required careful conditioning. Yaw angle data from the IMU were found to be sensitive to transient disturbances, especially due to thruster-induced vibration. GPS offered stable corrections, essential for global position updates, but could only function during surfaced intervals. The DVL was effective for tracking velocity but showed susceptibility to noise in shallow, reflective environments. Meanwhile, the depth sensor required re-zeroing to align with true sea-level references.

This experiment provided a crucial baseline for understanding sensor interactions during glider surface operations and demonstrated the importance of combining sensor strengths through a fusion algorithm to maintain accurate state estimation.

C. Submersion Test Result

The second scenario evaluated sensor behavior during a controlled dive and ascent maneuver. The vehicle was programmed to glide downward to a depth of approximately 3.5 meters before resurfacing. This test was critical for assessing the performance of the navigation system in GPS-denied environments and evaluating the capability of each sensor to contribute to accurate state estimation underwater.

The depth sensor performed reliably throughout the dive, capturing a smooth descent and ascent profile that closely matched the vehicle's trajectory (see Fig. 9). The sensor recorded a maximum depth of 3.5 meters, confirming that the HAUG followed the expected gliding path. However, when the vehicle was at the surface, the depth sensor consistently reported an offset of approximately −1 meter, which varied slightly over time. This offset was attributed to sensor calibration drift or minor ambient pressure variations at the water–air interface. To correct this, the navigation system applied zero-point correction using verified GPS data during surfaced intervals.

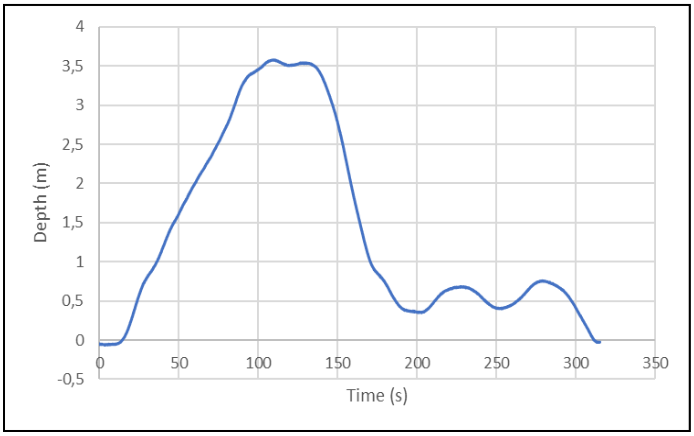

Figure 9. Depth measurement at submersion scenario

The IMU was instrumental in tracking the vehicle's orientation throughout the dive (see Fig. 10). The pitch angle varied significantly as the vehicle transitioned from level to nose-down and then back to level during resurfacing. Yaw and roll angles remained relatively stable, although a small persistent roll bias (~3°) was observed during this scenario, smaller than in the surface test. Notably, IMU acceleration data exhibited reduced noise compared to the surface motion (see Fig. 11). This is likely due to the absence of main thruster activation during the glide, eliminating vibration-induced interference. Nonetheless, gravitational effects continued to influence axis-specific readings, necessitating transformation into Earth coordinates during propagation.

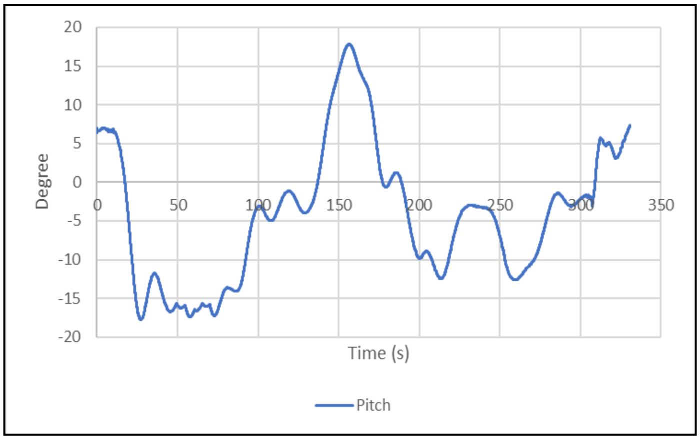

Figure 10. Pitch angle at submersion scenario

As anticipated, GPS data was unavailable during submersion (see Fig. 12). Signal loss occurred shortly after the dive began, and no valid position updates were received until the vehicle resurfaced. Upon reacquisition, the GPS sometimes returned brief anomalous spikes with unrealistic position jumps. These were automatically discarded using satellite count and covariance thresholds. The navigation system handled GPS signal loss by suspending position correction and relying solely on IMU and depth data for propagation. Once GPS became reliable again, it was used for resampling and correction.

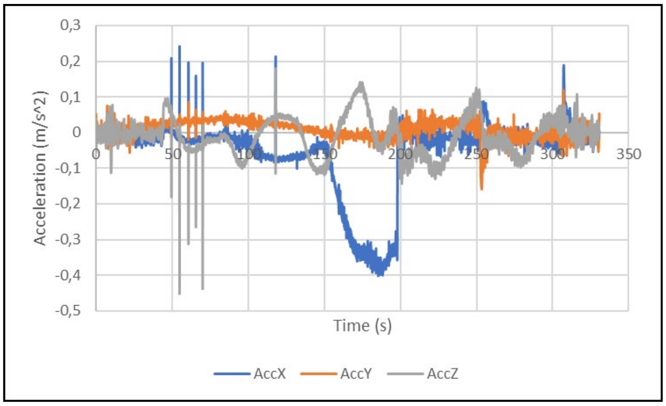

Figure 11. IMU's acceleration measurement at submersion scenario

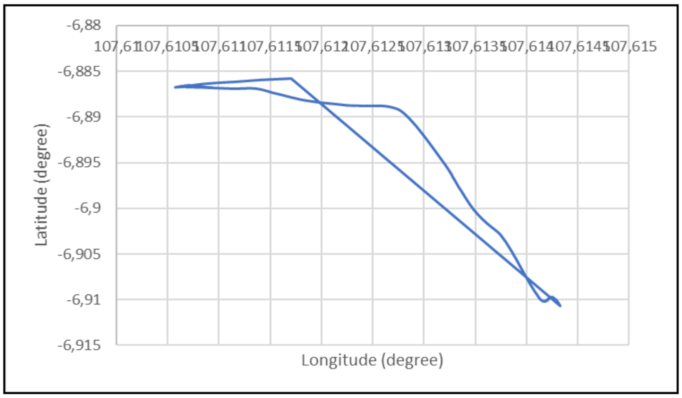

Figure 12. GPS's coordinate measurement at submersion scenario

The DVL, operating at 1 Hz, struggled to maintain bottom-lock in the relatively shallow test pool (see Fig. 13). The soft floor and limited depth often caused acoustic pings to scatter or reflect poorly, leading to intermittent or missing data. The vertical velocity channel was particularly noisy, and readings during the dive phase were deemed unreliable. In contrast, horizontal velocity was available intermittently and showed some consistency with the vehicle's motion. Due to the DVL's degraded performance, the system prioritized IMU and depth sensor data to infer vertical motion during the dive.

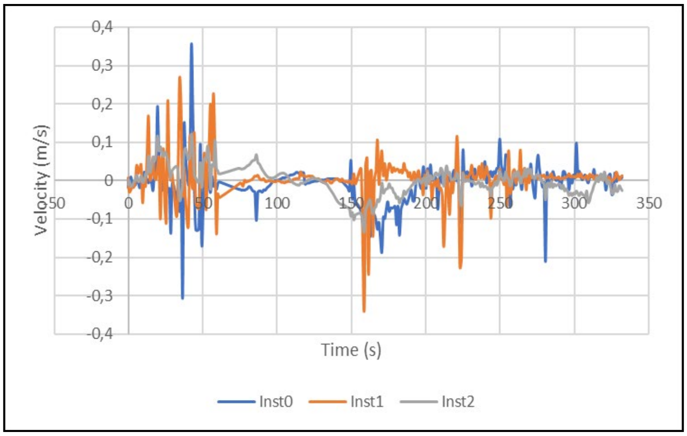

Figure 13. DVL's velocity measurement at submersion scenario

These submersion results demonstrate the challenges inherent in underwater navigation where GPS signals are unavailable, and bottom-referenced sensors like DVL are compromised by environmental limitations. The observations justified the system design decision to rely heavily on Particle Filter propagation using IMU-depth data during GPS outages, with conditional resampling when high-confidence sensor data becomes available.

D. Data Filtering

To ensure robust state estimation within the navigation system, sensor measurements underwent a series of preprocessing steps. These processes aimed to reduce noise, correct known biases, and flag or discard unreliable data prior to their integration within the Particle Filter framework. Each sensor type was treated with tailored strategies based on its characteristics and the operational conditions encountered during testing.

D.1 Inertial Measurement Unit (IMU)

Raw acceleration and angular velocity data from the IMU were sampled at 40 Hz. These signals exhibited high-frequency noise primarily induced by the main thruster, especially during surface operations. To mitigate this, a low-pass Butterworth filter was applied to isolate true motion components from vibration. Furthermore, orientation estimates (roll, pitch, yaw) were smoothed using a moving average filter to suppress transient oscillations.
Notably, a roll angle bias of approximately 13° was observed during surface motion, and 3° during submerged operation. These static offsets, possibly due to mounting asymmetry or sensor miscalibration, were recorded and compensated during the resampling phase of the Particle Filter. The effect of filtering is visualized in (see Fig. 14), which compares raw and filtered IMU acceleration signals.

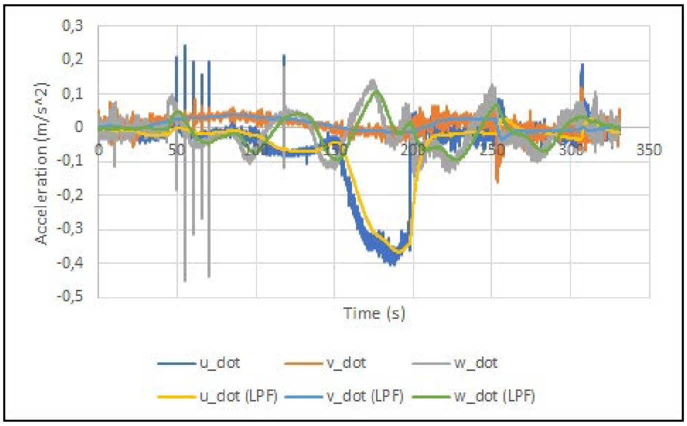

Figure 14. Raw and filtered IMU acceleration signals comparation

D.2 Global Positioning System (GPS)

GPS data, available only during surfaced phases, provided ground-truth references for horizontal position. However, reacquisition after submersion often introduced brief spikes or jump artifacts due to low satellite count or high covariance. Therefore, a validation routine was implemented:

- Fixes with fewer than 5 satellites or with covariance above a predefined threshold were discarded.
- Only validated data were used to trigger Particle Filter resampling.

Figure (see Fig. 15) illustrates a sample GPS trajectory where valid points (blue) and rejected spikes (orange) are clearly distinguished.

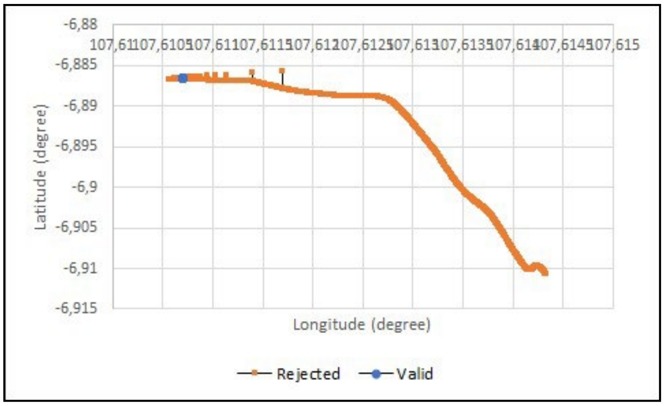

Figure 15. GPS valid and rejected spikes

D.3 Doppler Velocity Log (DVL)

DVL provided 3-axis velocity data at 1 Hz. During surface motion, bottom-lock was reliable, but during submersion, especially in shallow water or over soft pool surfaces, bottom-lock failures occurred, causing intermittent velocity dropout and noisy vertical velocity. All DVL channels were passed through a second-order Butterworth low-pass filter to remove acoustic noise.

Data points without bottom-lock confirmation were either excluded or interpolated if within a short gap window. A filtered velocity trace with bottom-lock indicators is shown in (see Fig. 16).

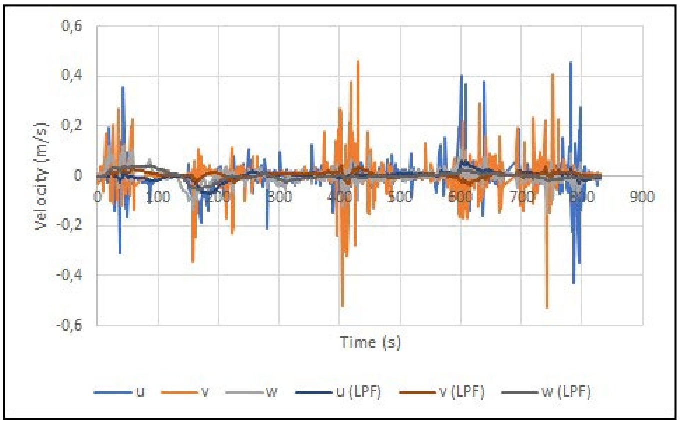

Figure 16. Filtered velocity trace

D.4 Depth Sensor

The pressure-based depth sensor produced consistent measurements at 10 Hz. However, a constant surface offset of approximately −1 meter was observed. This offset was environmentally dependent and slightly variable across tests.

A surface correction routine was implemented: when GPS confirmed the vehicle was at the surface (and no active thruster input was detected), the depth was reset to 0. In addition, a simple moving average filter smoothed out minor jitter during glides, improving vertical localization stability. Fig. 17 shows the depth signal before and after zero-level correction.

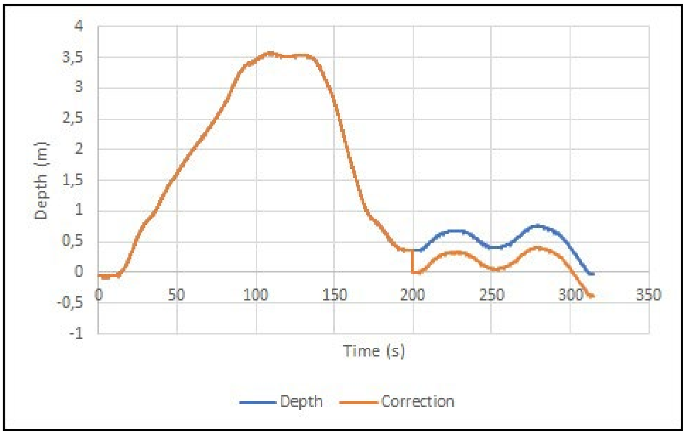

Figure 17. Before and after zero-level correction

E. Summary of Sensor Behavior

To consolidate the findings from both the surface and submersion scenarios, a summary of sensor performance is provided. Each sensor was assessed based on its accuracy, availability, noise characteristics, and reliability under different operating conditions. These criteria are crucial for informing sensor selection and weighting strategies in the navigation system.

Table 1. Summary of Sensor Behavior Based on Test

Sensor	Accuracy	Availability	Noise Level	Observations
IMU	Moderate (orientation consistent)	Continuous	High (surface), Low (submerged)	Sensitive to thruster vibrations; requires low-pass filtering and bias correction.
GPS	High (when available)	Surface only	Low	Essential for global corrections; subject to reacquisition delay and covariance filtering.
DVL	High (when bottom-lock maintained)	Intermittent	Moderate to High	Effective on solid seabeds; unreliable in shallow water or soft-bottom conditions.
Depth	High	Continuous	Low	Stable during descent/ascent; requires surface offset correction.

The IMU consistently provided orientation and acceleration data across all phases, but its signals were particularly noisy during surface operation due to actuator-induced vibration. Filtering improved its usability, and orientation estimates were deemed sufficiently stable after bias adjustment.

GPS, while highly accurate, was only available during surface operations. It was critical for correcting accumulated drift but required preprocessing to remove outliers and invalid fixes. Its role in Particle Filter resampling was pivotal during re-emergence from submersion.

The DVL contributed accurate velocity data only when bottom-lock was maintained. However, in the shallow pool environment, frequent lock loss and vertical velocity dropout limited its utility. In deeper and more structured seabeds, DVL is expected to perform better.

Depth sensors were reliable and consistent throughout both test scenarios, with only a minor and correctable surface offset. Their high resolution and low noise made them ideal for vertical localization, especially during submerged operation.

Overall, no single sensor could independently support the navigation system across all mission phases. The relative strengths and weaknesses necessitated a fusion strategy that adapts to sensor availability and trustworthiness over time. The system leveraged IMU and depth data for continuous propagation and GPS/DVL measurements for opportunistic corrections.

This sensor evaluation supports the design choice of using a Particle Filter, which inherently accommodates varying measurement uncertainties and intermittent observation windows.

4. Navigation System Design

The navigation system for the Hybrid Autonomous Underwater Glider (HAUG) is designed to estimate the vehicle's position and velocity accurately by fusing information from multiple onboard sensors. This section details the architecture of the navigation framework, the algorithmic flow of the Particle Filter, and the integration strategy for sensor measurements.
Navigation-Guidance-Control (NGC) Framework

Fig. 18 presents the structure of the integrated Navigation-Guidance-Control (NGC) system implemented on the HAUG. The navigation module is responsible for estimating the current state (position and velocity) based on sensor inputs. The guidance module provides desired setpoints or waypoints for the mission, and the control module generates appropriate actuator commands to follow the trajectory.

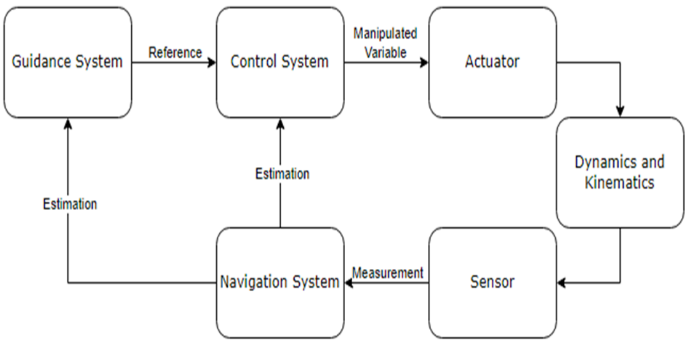

Figure 18. Block diagram of the Navigation-Guidance-Control system

The estimation output from the navigation system is fed into the guidance module, which determines heading and depth targets. These targets are then converted into actuator commands by the control system, which adjusts the glider's pitch, roll, or thrust accordingly. This closed-loop operation allows for autonomous movement along a desired path.

B. Navigation Subsystem Architecture

The navigation subsystem was implemented using a Particle Filter-based estimation algorithm. Sensor inputs include:

- IMU: linear acceleration, angular velocity, orientation (40 Hz)
- DVL: 3-axis velocity relative to seafloor (1 Hz)
- Depth sensor: vertical position (10 Hz)
- GPS: absolute position (when surfaced, 40 Hz)

These sensor inputs are processed through data conditioning pipelines and then fed into the Particle Filter algorithm for state estimation. Fig. 19 illustrates the subsystem block diagram of the navigation design.

The estimated state vector includes 3D position in the NED frame and 3D velocity in the body frame. This state vector is continuously updated even when some sensor inputs are missing, such as during submerged operation.

The Particle Filter (PF)-based navigation algorithm was implemented on an embedded Linux platform using an NVIDIA Jetson Nano, which features a quad-core ARM Cortex-A57 CPU and 4 GB RAM. With 50 particles, the system achieved an update rate of 8–10 Hz, while resampling operations consumed approximately 30 ms per cycle. Sensor inputs—IMU (40 Hz), depth sensor (10 Hz), GPS (40 Hz when surfaced), and DVL (1 Hz)—were processed asynchronously. This configuration provided sufficient computational throughput for real-time navigation without requiring high-performance hardware. Power consumption during active operation averaged 4.3 W, which aligns with HAUG's energy budget for submerged and hybrid gliding missions. While the current setup is sufficient for short to medium-duration deployments, increasing the number of particles or adding heavier computation (e.g., terrain-relative updates) would raise both power demand and CPU usage.

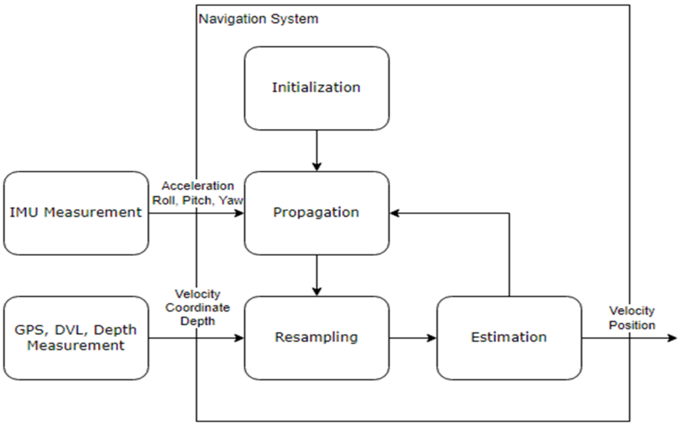

Figure 19. Navigation system architecture based on particle filter algorithm

C. Navigation Algorithm Description

The navigation algorithm is based on a Sequential Monte Carlo (SMC) Particle Filter. The design includes three main stages:

C.1 Initialization

A cloud of particles is initialized to represent possible states $[x_i, y_i, z_i, u_i, v_i, w_i]$, where each particle has a weight w_i. Initial distributions are based on available GPS and depth data or set manually if unavailable.

$initialization(N)$:

$P = \emptyset$

$X_0 = [\boldsymbol{\eta}_0 \quad \boldsymbol{v}_0]^T = [[x_0 \quad y_0 \quad z_0]^T \quad [u_0 \quad v_0 \quad w_0]^T]^T$

$for\ i = 1, \ldots, N$

$X^{(i)} \sim p(X_0)$

$P \cup X^{(i)}$

$return\ P$

Figure 20. Particle filter initialization algorithm

C.2 Propagation

During propagation, particles are updated using the kinematic motion model. Acceleration and orientation from the IMU are used to update the velocity in the body frame, which is then transformed into Earth coordinates using rotation matrices based on Euler angles.

$propagation(P, \boldsymbol{z_{IMU}}, \boldsymbol{z_{RPY}})$:

$\tilde{P} = \emptyset$

$for\ i = 1, \dots, N$

$\boldsymbol{v_{k+1}}^{(i)} = \boldsymbol{v_k}^{(i)} + \boldsymbol{z_{IMU}} * dt + random()$

$\dot{\boldsymbol{\eta}}_{\boldsymbol{k+1}}^{(i)} = R(\boldsymbol{z_{RPY}})\boldsymbol{v_{k+1}}^{(i)}$

$\boldsymbol{\eta_{k+1}}^{(i)} = \boldsymbol{\eta_k}^{(i)} + \dot{\boldsymbol{\eta}}_{\boldsymbol{k+1}}^{(i)} * dt$

$\tilde{P} \cup [\boldsymbol{v_{k+1}}^{(i)} \quad \boldsymbol{\eta_{k+1}}^{(i)}]^T$

$return\ \tilde{P}$

Figure 21. Propagation stage using IMU-based motion model

C.3 Resampling

The Particle Filter updates particle weights based on the likelihood of sensor observations. GPS (North-East), DVL (velocity), and depth sensor (z-axis) data are used. Measurement likelihoods are modeled using Gaussian distributions centered at observed values, with standard deviations derived from calibration.

The Particle Filter implementation in this work adopts a modular resampling scheme tailored to the selective availability of sensor measurements. Each particle maintains a six-degree-of-freedom (6-DoF) state vector comprising position (*x, y, z*) and velocity (*u, v, w*). When new measurements arrive, only the subspace corresponding to the observed modality is resampled, while the remaining dimensions are preserved.

Specifically, when GPS data is available, the *x* and *y* position components of the particle set are resampled based on measurement likelihood. Similarly, if depth sensor data is available, the *z* component undergoes resampling. When valid DVL measurements are received, the velocity components *u, v, w* are resampled accordingly. These partial updates result in separate particle sets (*Pxy, Pz, Pv*), each resampled with respect to its specific observation. The operation denoted as *merge* then consolidates these component-wise particle sets into a unified 6-DoF particle set *P*, ensuring each particle contains updated values for all dimensions. This strategy maintains consistency while avoiding redundant computation and helps mitigate degeneracy through focused likelihood evaluations.

$resampling(\tilde{P}, \boldsymbol{z_{GPS}}, \boldsymbol{z_{DVL}}, \boldsymbol{z_{Depth}})$:

$if(\boldsymbol{z_{GPS}} = \emptyset)$: GPS measurement not available

$P_{xy} = \tilde{P}_{xy}$

$else\ if(\boldsymbol{z_{GPS}} \neq \emptyset)$: GPS measurement available

$P_{xy} = \emptyset$

$w_{GPS} = \emptyset$

$for\ i = 1, \dots, N$

$\boldsymbol{w_k}^{(i)} \sim P([x_k{}^{(i)} \quad y_k{}^{(i)}] | \boldsymbol{z_{GPS}})$

$w_{GPS} \cup \boldsymbol{w_k}^{(i)}$

$P_{xy} = resample(\tilde{P}_{xy}, w_{GPS})$

$if(z_{Depth} = \emptyset)$: Depth measurement not available

$P_z = \tilde{P}_z$

$else\ if(z_{Depth} \neq \emptyset)$: Depth measurement available

$P_z = \emptyset$

$w_{Depth} = \emptyset$

$for\ i = 1, \dots, N$

$w_k{}^{(i)} \sim P(z_k{}^{(i)} | z_{Depth})$

$w_{Depth} \cup w_k{}^{(i)}$

$P_z = resample(\tilde{P}_z, w_{Depth})$

$if(\boldsymbol{z_{DVL}} = \emptyset)$: DVL measurement not available

$P_v = \tilde{P}_v$

$else\ if(\boldsymbol{z_{DVL}} \neq \emptyset)$: DVL measurement available

$P_v = \emptyset$

$w_{DVL} = \emptyset$

$for\ i = 1, \dots, N$

$\boldsymbol{w_k}{}^{(i)} \sim P(\boldsymbol{v_k}{}^{(i)} | \boldsymbol{z_{DVL}})$

$w_{DVL} \cup \boldsymbol{w_k}{}^{(i)}$

$P_v = resample(\tilde{P}_v, w_{DVL})$

$P = merge(P_{xy}, P_z, P_v)$

$return\ P$

Figure 22. Sensor fusion and resampling strategy

D. Handling Sensor Dropout

One of the critical advantages of the Particle Filter is its ability to handle intermittent or missing data:

- When GPS is unavailable (e.g., submerged), state prediction continues using IMU and DVL.
- When DVL bottom-lock is lost, propagation relies on IMU, and resampling is skipped until new measurements are available.
- If depth sensor fails temporarily, a confidence-based prediction continues using vertical acceleration and buoyancy data.

This flexible framework allows the system to maintain continuity of estimation even in challenging underwater conditions. The Particle Filter output is the estimated state vector at every timestep, including:

- Position: x, y, z in the Earth-fixed NED frame
- Velocity: u, v, w in the vehicle's body frame

These estimates are used by the guidance module to compare against the next waypoint and compute navigation errors. The navigation system updates its output at a frequency of 10 Hz, with resampling triggered adaptively based on sensor input availability and weight variance.

E. Motion Mode Generalization and Energy-Aware Estimation

The proposed Particle Filter (PF) employs a kinematics-based state propagation model that is agnostic to specific vehicle actuation mechanisms. It uses inertial inputs (e.g., linear acceleration and orientation) to update position and velocity estimates, without relying on vehicle-specific dynamic parameters such as thrust profiles or buoyancy models. This abstraction allows the method to generalize across various underwater platforms—including gliders, hybrid vehicles, and conventional AUVs—making it broadly applicable in GPS-denied underwater environments.

During motion mode transitions, such as from powered propulsion to buoyancy-driven glide, the PF continues to propagate using consistent kinematic equations, ensuring seamless estimation continuity. The algorithm's modular structure supports asynchronous sensor updates and allows for adaptive resampling based on sensor availability and particle weight variance. These features make the system energy-aware by reducing computational overhead during low-dynamic phases, and robust by maintaining state estimates during intermittent sensor dropout. The resulting framework is well-suited for long-duration missions across different classes of autonomous underwater vehicles.

F. Particle Filter Modifications for Underwater Navigation

To improve the robustness and accuracy of state estimation in underwater environments, several modifications were incorporated into the standard Particle Filter framework. First, an adaptive resampling mechanism was employed, wherein resampling is not performed at fixed intervals but is instead triggered opportunistically—whenever high-confidence sensor measurements (e.g., GPS, DVL, or depth) become available. This reduces unnecessary computational load and mitigates sample impoverishment during periods of limited observability.

In addition, a particle rejuvenation mechanism was introduced to handle cases where the current particle distribution significantly diverges from new sensor measurements. When reliable observations are available but deviate substantially from the estimated belief, a portion of the particle set is reinitialized based on the new measurements. This targeted reinitialization helps recover from filter divergence and improves tracking performance following sudden changes in vehicle motion or unexpected external disturbances. These modifications, while lightweight, enhance the filter's ability to maintain consistent state estimation in the presence of intermittent sensor dropout and underwater uncertainty.

5. Experimental Assessment of Navigation System

To validate the proposed navigation system, field experiments were conducted using the HAUG prototype at Pangandaran Beach (see Fig. 23), Indonesia. These experiments aimed to evaluate the accuracy and robustness of the Particle Filter algorithm under real-world conditions, particularly focusing on GPS-denied operation, sensor dropout, and actuator disturbances.

Figure 23. Field testing at Pangandaran beach

A. Test Environment and Motion Profile

The test was conducted in a nearshore environment with calm water and a sloping seabed. The HAUG vehicle was configured to execute a waypoint-based path on the surface and undergo brief submersion cycles as part of its hybrid control strategy.

Fig. 24 illustrates the pitch angle profile throughout the test. Notable downward spikes correspond to moments when the vehicle initiated a glide motion, resulting in submersion. These pitch variations were triggered by changes in buoyancy and moving mass to achieve descent angles.

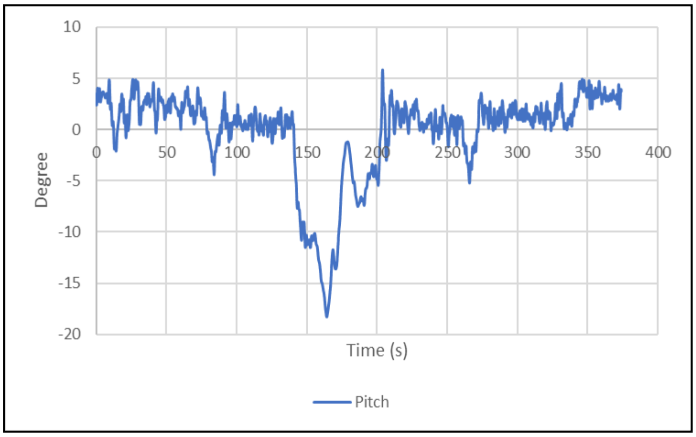

Figure 24. Pitch angle measurements showing submersion cycles during navigation test

Fig. 25 presents the yaw angle (heading) measurements. Each sharp transition indicates a switch to a new waypoint. The transitions were mostly smooth, although minor oscillations are present due to inertial overshoot and hydrodynamic disturbances, which the control system partially corrected.

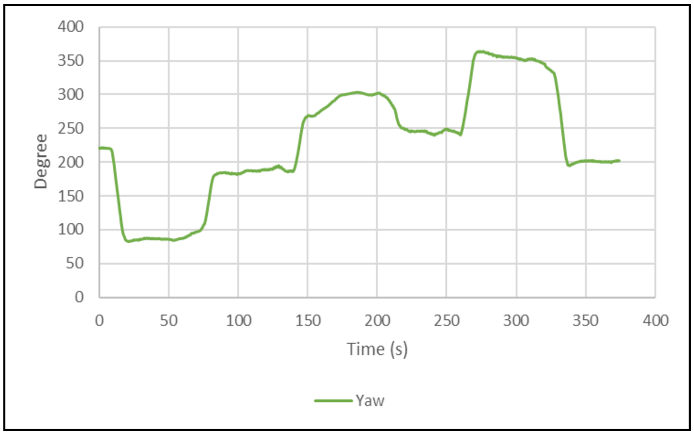

Figure 25. Yaw angle changes during surface navigation based on waypoint commands

B. Position and Depth Estimation Behavior

Fig. 26 displays the GPS-measured trajectory overlaid with gaps where the vehicle was submerged. During these submerged intervals, the Particle Filter continued propagating the estimated state using IMU and depth data alone. Noticeable drift is visible in the estimated track during those gaps, but correction occurs upon GPS reacquisition.

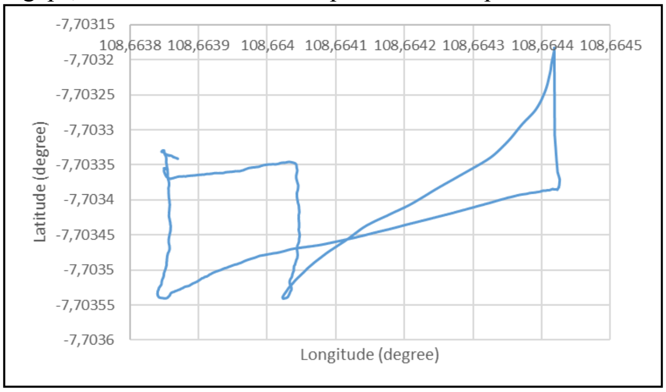

Figure 26. GPS trajectory with visible displacement and correction after submersion phases

Depth readings from the onboard pressure sensor are shown in Fig. 27. The glider achieved a maximum depth of 3.5 meters before resurfacing. An initial surface offset (~1.5 m) was noted and later compensated in the navigation model. Depth transitions were smooth, demonstrating the effectiveness of the buoyancy system in achieving vertical motion.

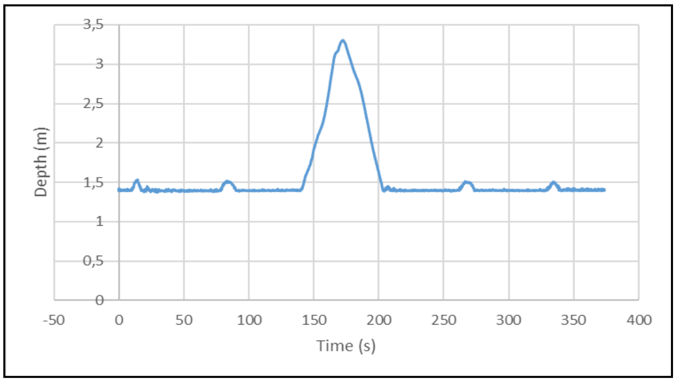

Figure 27. Measured depth profile showing glide descent and resurfacing patterns

C. Velocity and Acceleration Estimation

Velocity estimates from the Particle Filter are shown in Fig. 28, where forward (surge) velocity varied between 0 and 1.2 m/s. The velocity sharply decreased during submersion when the thruster was turned off, then increased again upon surfacing and reactivation. This pattern confirms proper synchronization between navigation and control modules.

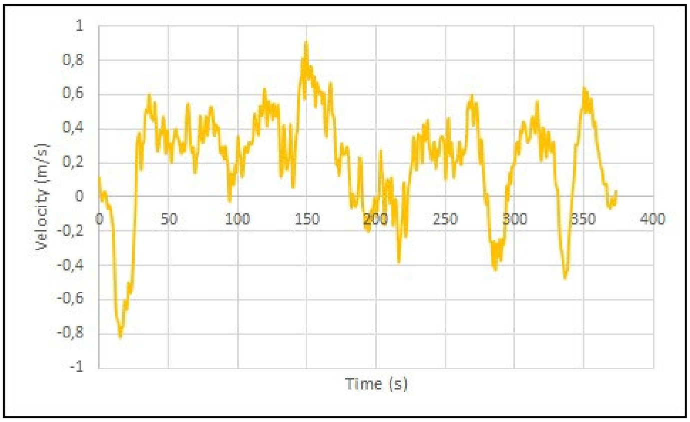

Figure 28. Estimated forward velocity (surge) of the vehicle during the mission

Fig. 29 presents IMU-derived acceleration readings along the vehicle's forward axis. The acceleration profile is noisy during active propulsion but stabilizes when the thruster is disabled. This further validates the hypothesis that thruster-induced vibration interferes with inertial measurements and justifies the use of low-pass filtering during preprocessing.

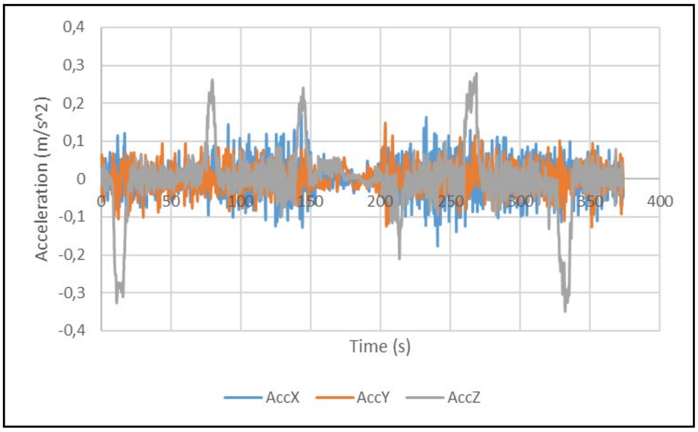

Figure 29. IMU acceleration data showing noise increase during thruster activation

D. Navigation Accuracy and Filter Response

Fig. 30 compares the estimated position from the Particle Filter against available GPS measurements. During submerged phases, the estimation followed a consistent trajectory without abrupt divergence, and alignment with GPS improved after resurfacing. This supports the ability of the system to maintain coherence without GPS and perform correction during resampling.

In absence of underwater ground-truth, GPS-based loop closures were used during surface intervals to validate positional consistency. In future work, acoustic beacons or visual odometry may provide submerged ground-truth references.

After GPS reacquisition, the difference between estimated and measured positions was used to evaluate Particle Filter performance. The average deviation was under 2.5 meters per surfacing.

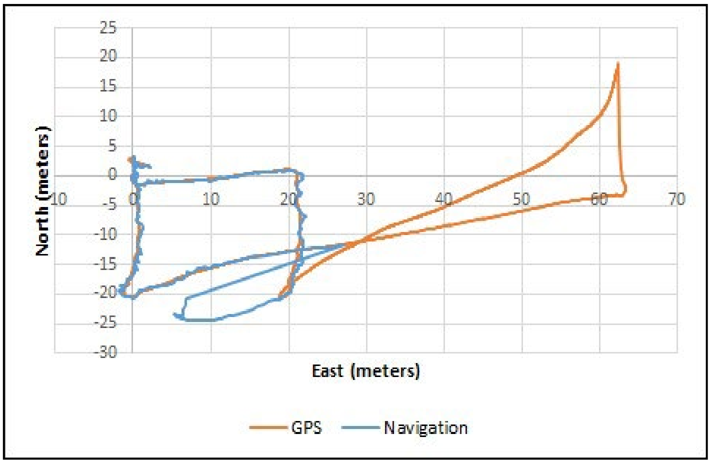

Figure 30. Comparison between estimated position and GPS measurements (surfaced phases only)

Similarly, Fig. 31 compares the estimated depth from the Particle Filter to the raw pressure sensor data. Minor deviations are observable due to integration noise and IMU-induced drift, but the Particle Filter maintained a reasonable depth trajectory, especially during transitions.

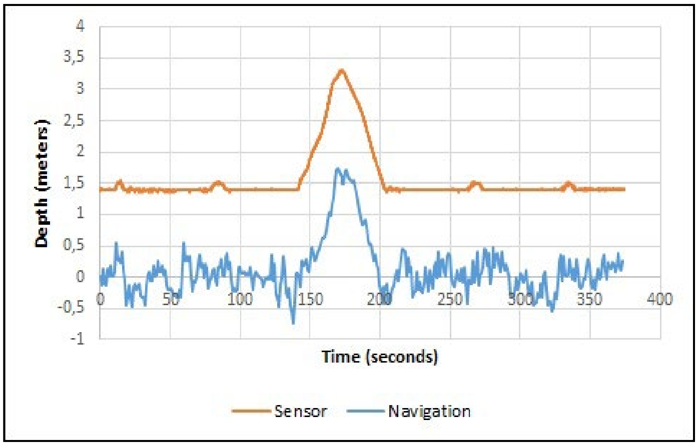

Figure 31. Comparison between estimated depth and raw depth sensor data

Finally, Fig. 32 displays the body-frame velocity estimates in all three axes (surge, sway, heave). Surge dominates during propulsion; sway remains near zero, while heave oscillates during pitch maneuvers and vertical transitions.

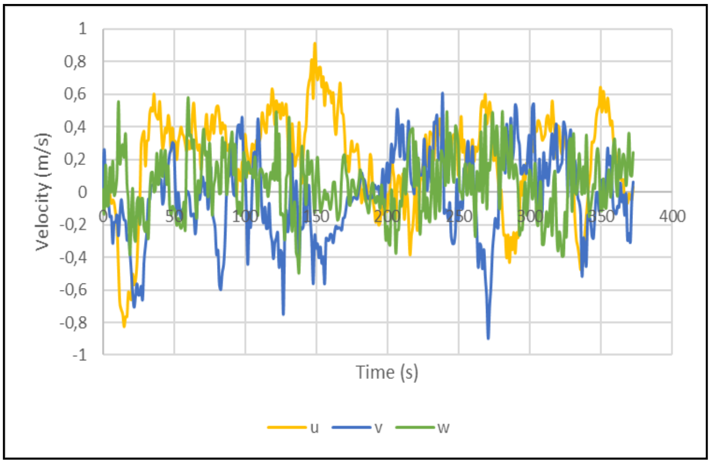

Figure 32. Estimated body-frame velocity in surge, sway, and heave directions

These tests were conducted under typical coastal disturbances, including soft-bottom seabeds, intermittent GPS availability, and acoustic noise, providing a realistic evaluation of filter robustness.

E. Discussion
These experimental results demonstrate that the navigation system performs well under constrained conditions:

- The Particle Filter was able to propagate state accurately during GPS unavailability, thanks to IMU and depth integration.
- Resampling and correction were successfully triggered upon GPS reacquisition, preventing long-term drift.
- Thruster activation introduces measurable noise to both IMU and DVL signals, highlighting the need for better mechanical isolation or advanced filtering.
- The system proved robust against sensor dropout, with no failure in state estimation or need for reinitialization.

These findings validate the feasibility of using a Particle Filter-based architecture for autonomous underwater navigation in hybrid glider operations.

While the current work does not include quantitative comparisons against alternative filters such as the Extended Kalman Filter (EKF) or Unscented Kalman Filter (UKF), preliminary investigations suggest that Particle Filters offer improved robustness in nonlinear and GPS-denied conditions typical of underwater environments. However, due to the lack of full ground-truth trajectories and the complexity of deploying reference localization systems in field trials, formal RMSE metrics could not be computed. Instead, loop-closure comparisons using surface GPS fixes were utilized as qualitative proxies to assess estimation consistency. In future work, we intend to incorporate acoustic beacon systems or visual-based reference localization to enable quantitative performance benchmarking, including RMSE and standard deviation against known ground truth. Additionally, side-by-side simulations with EKF/UKF implementations will be pursued to provide comparative insights into estimation accuracy, stability, and computational trade-offs.

6. Conclusion

This paper has presented the design and experimental validation of a navigation system for a Hybrid Autonomous Underwater Glider (HAUG) using a Particle Filter-based estimation framework. The system was developed to address the inherent challenges of underwater navigation in GPS-denied environments by fusing measurements from an Inertial Measurement Unit (IMU), Doppler Velocity Log (DVL), depth sensor, and GPS (when surfaced).

A series of experiments were conducted in a controlled coastal environment to evaluate the system's performance under realistic operational conditions. The results demonstrate that the Particle Filter-based navigation system can maintain accurate and consistent estimates of position and velocity during both surfaced and submerged phases. The algorithm exhibited robustness in the face of sensor dropout, actuator-induced disturbances, and non-linear vehicle dynamics. GPS-based corrections successfully constrained long-term drift, while depth and DVL data improved local consistency and accuracy.

Additionally, analysis of sensor behavior highlighted the importance of data conditioning, especially in the presence of thruster-induced noise. The system's ability to continue state propagation during sensor unavailability and resume resampling upon re-acquisition further underscores its resilience and suitability for hybrid underwater missions.

Due to the lack of continuous ground-truth references (e.g., secondary GPS or external tracking), quantitative uncertainty metrics such as RMSE or confidence bounds could not be computed directly. However, GPS-based loop closure during resurfacing indicates a mean positional correction below 2.5 meters. Across multiple dive-glide cycles, estimated positions upon resurfacing consistently aligned within a few meters of GPS updates, suggesting limited drift during submerged navigation. Further quantitative evaluation will be pursued in future work using external acoustic localization or visual tracking systems.

Future work will focus on extending this framework to three-dimensional path planning and closed-loop trajectory control, as well as testing in deeper and more complex underwater terrains. Integration with terrain-relative navigation (TRN) and acoustic localization methods may further improve accuracy in fully submerged operations without GPS access.

In future work, the navigation framework could be extended with additional sensing modalities, such as forward-looking sonar, terrain-aided navigation maps, or acoustic beacon systems. These complementary sources may improve localization in fully GPS-denied environments and reduce drift in long-duration submerged operations. Furthermore, non-traditional integration methods, such as map-matching or collaborative multi-AUV localization, may enhance robustness and provide situational awareness beyond onboard sensing. Future work will also involve benchmarking with EKF/UKF filters under identical conditions, and integration of acoustic/visual ground-truth systems to provide formal RMSE evaluation.

7. References

[1]. P. Liu, B. Wang, Z. Deng, and M. Fu, "INS/DVL/PS Tightly Coupled Underwater Navigation Method with Limited DVL Measurements," *IEEE Sens. J.*, vol. 18, no. 7, pp. 2994–3002, 2018, doi: 10.1109/JSEN.2018.2800165.

[2]. F. S. Dubrovin and A. F. Scherbatyuk, "Studying some algorithms for AUV navigation using a single beacon: The results of simulation and sea trials," *Gyroscopy Navig.*, vol. 7, no. 2, pp. 189–196, 2016, doi: 10.1134/S2075108716020024.

[3]. S. A. Imtiaz, K. Roy, B. Huang, S. L. Shah, and P. Jampana, "Estimation of states of nonlinear systems using a particle filter," *Proc. IEEE Int. Conf. Ind. Technol.*, no. May 2014, pp. 2432–2437, 2006, doi: 10.1109/ICIT.2006.372687.

[4]. J. Elfring, E. Torta, and R. van de Molengraft, "Particle Filters: A Hands-On Tutorial," *Sensors*, vol. 21, no. 2, p. 438, Jan. 2021, doi: 10.3390/s21020438.

[5]. F. Maurelli, S. Krupińskiy, Y. Petillot, and J. Salviz, "A particle filter approach for AUV localization," *Ocean. 2008*, no. May 2014, 2008, doi: 10.1109/OCEANS.2008.5152014.

[6]. N. Osterman and C. Rhen, "Exploring the sensor requirements for particle filter-based terrain-aided navigation in AUVs," *2020 IEEE/OES Auton. Underw. Veh. Symp. AUV 2020*, no. Dvl, pp. 25–30, 2020, doi: 10.1109/AUV50043.2020.9267886.

[7]. B. V. Menna, S. A. Villar, and G. G. Acosta, “Particle Filter based Autonomous Underwater Vehicle Navigation System aided thru acoustic communication ranging,” *2020 Glob. Ocean. 2020 Singapore - U.S. Gulf Coast*, 2020, doi: 10.1109/IEEECONF38699.2020.9389432.
[8]. T. I. Fossen, *Handbook of Marine Craft Hydrodynamics and Motion Control*. Wiley, 2011.
[9]. P. Wu, W. Nie, Y. Liu, and T. Xu, “Improving the underwater navigation performance of an IMU with acoustic long baseline calibration,” *Satell. Navig.*, vol. 5, no. 1, pp. 1–16, 2024, doi: 10.1186/s43020-023-00126-1.
[10]. F. C. Teixeira, J. Quintas, and A. Pascoal, “AUV terrain-aided navigation using a doppler velocity logger,” *IFAC-PapersOnLine*, vol. 28, no. 2, pp. 137–142, 2015, doi: 10.1016/j.ifacol.2015.06.022.
[11]. X. Bo, A. A. Razzaqi, and G. Farid, “A review on optimal placement of sensors for cooperative localization of AUVs,” *J. Sensors*, vol. 2019, 2019, doi: 10.1155/2019/4276987.
[12]. M. S. M. Aras *et al.*, “Analysis of integrated sensors for unmanned underwater vehicle application,” *USYS 2016 - 2016 IEEE 6th Int. Conf. Underw. Syst. Technol. Theory Appl.*, pp. 224–229, 2017, doi: 10.1109/USYS.2016.7893914.
[13]. M. Dinc and C. Hajiyev, “Integration of navigation systems for autonomous underwater vehicles,” *J. Mar. Eng. Technol.*, vol. 14, no. 1, pp. 32–43, 2015, doi: 10.1080/20464177.2015.1022382.
[14]. G. Taraldsen, T. A. Reinen, and T. Berg, “The underwater GPS problem,” *Ocean. 2011 IEEE - Spain*, pp. 1–8, 2011, doi: 10.1109/Oceans-Spain.2011.6003649.
[15]. S. Siregar *et al.*, “Design and Construction of Hybrid Autonomous Underwater Glider for Underwater Research,” *Robotics*, vol. 12, no. 1, p. 8, Jan. 2023, doi: 10.3390/robotics12010008.
[16]. F. Gustafsson, “Particle filter theory and practice with positioning applications,” *IEEE Aerosp. Electron. Syst. Mag.*, vol. 25, no. 7 PART 2, pp. 53–81, 2010, doi: 10.1109/MAES.2010.5546308.
[17]. J. J. Leonard and A. Bahr, “Autonomous Underwater Vehicle Navigation,” in *Springer Handbook of Ocean Engineering*, no. February, Cham: Springer International Publishing, 2016, pp. 341–358.

Natsir Habibullah received the bachelor’s degree in Physical Engineering from Institut Teknologi Bandung (ITB), the master's degree in Electrical Engineering from Institut Teknologi Bandung (ITB). Currently, he is a doctoral candidate in electrical engineering at Institut Teknologi Bandung (ITB). His research interests include modeling and system identification, system navigation, guidance, and control, as well as the Internet of Things.

Bambang Riyanto Trilaksono received the bachelor’s degree in electrical engineering from Institut Teknologi Bandung, Bandung, Indonesia, and the master’s and Ph.D. degrees in electrical engineering from Waseda University, Tokyo, Japan. He is currently a Professor with the Control and Computer System Research Group, School of Electrical Engineering and Informatics, Institut Teknologi Bandung. His research interests include control systems, robotics, and artificial intelligence.

Egi Muhammad Idris Hidayat received the bachelor's degree in electrical engineering from Institut Teknologi Bandung (ITB), the M.Sc. degree in control and information systems from Universitat Duisburg-Essen, and the Ph.D. degree in electrical engineering from Uppsala University. Currently, he is a Lecturer at the School of Electrical Engineering and Informatics, ITB. His research interests include modeling and system identification, control and learning, and robotics.

Widyawardana Adiprawita received the degree in electrical engineering, the master's degree in informatics engineering, and the Ph.D. degree in electrical engineering from the Institut Teknologi Bandung (ITB), Bandung, Indonesia, in 1997, 2000, and 2011, respectively. Currently an Assistant Professor with the School of Electrical Engineering and Informatics, ITB. He has written more than 50 articles published in international publications. His research interests include embedded systems, robotics, computer vision, and artificial intelligence.

Simon Siregar received the bachelor's degree in Physics from Padjadjaran University, the master's degree in Electrical Engineering and Ph.D. degree in Electrical Engineering and Informatics from Institut Teknologi Bandung (ITB). Currently, he holds the position of Assistant Professor within the Department of Computer Engineering at the Faculty of Applied Science, Telkom University. His research endeavors are focused on the formal domains of modeling and system navigation, guidance, and control, with additional emphasis on image processing, artificial intelligence, and the Internet of Things (IoT).